FLOW CONTROL DOWNSTREAM OF A BACKWARD FACING STEP

P. G. SPAZZINI , G. IUSO , N. ZURLO , G. M. DI CICCA , M. ONORATO
CNR - CSDF c/o DIASP, Politecnico di Torino &
DIASP, Politecnico di Torino
C.so Duca degli Abruzzi, 24 - I 10129 Torino (ITALY)

Keywords: *Separation, Control, Backfacing Step, LEBU*

Abstract

A simple LEBU-like device aimed at controlling the separated flow field behind a backward facing step, with special attention on its unsteady properties, is described; the device advantage is that it requires very small design modifications and/or complications. Visualizations of the controlled field are presented along with wall hot-wire measurements. The latter measurements provided information about both the mean wall quantities (skin friction) and unsteady properties (wall shear stress fluctuations); RMS and spectra of these fluctuations are presented, showing how the distribution of fluctuation energy is influenced by the presence of the manipulator. In particular, specific positionings of the device allowed to reduce wall unsteadinesses. To summarize the outcomes of the work, although the research is in its early stages, the results presented here prove the viability of this way of controlling separated flows.

1 Introduction

The backfacing step (BFS) flow is an appropriate test case for real-life separated flows because of several reasons. It shows essentially all the flow features of the practical engineering applications where separation and reattachment occur; moreover, the geometry is very simple and easily reproducible. Further-

more, the separation point is *fixed*, which reduces greatly the experimental difficulties and the measurement uncertainties. A schematic of the flow topology is represented in fig. 1.
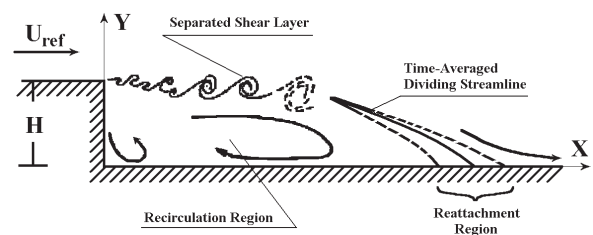

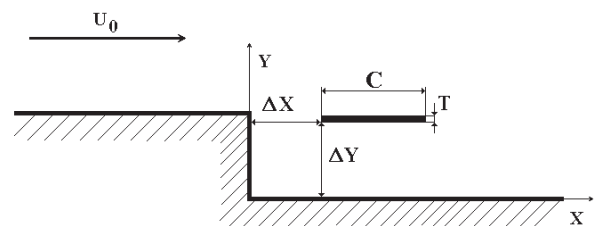**Fig. 1** Schematic of BFS flow topology

Fig. 2 Schematic of the flow control device

Most of the engineering problems that are posed by separating flow are associated with the high increase in dissipation and thus in aerodynamic drag and with the consequences of the stress fluctuations caused by the high level of unsteadiness that characterizes this class of flows. The latter effect, in particular, can bring to various undesirable phenom-

ena like fatigue ruptures or collapses due to excitation at some resonant frequencies of the structures bounding the separated region.

An important technological outcome of the basic research on separated flows is thus related with studies about methods aimed at controlling the unsteadiness around the separated region.

Several authors (see e.g. [2, 5, 16]) have worked on the separated flow downstream a step, evidencing several aspects of the problem related with the mean flow structure and with the unsteadiness of this kind of flow. About this last point, investigations indicate the contemporary presence of at least two instability sources, namely the vortex shedding from the primary separation point and a low frequency motion of the whole separated region, called 'flapping'. These phenomena produce unsteadiness on two frequency fields, separated by roughly one order of magnitude. Despite the important difference in frequencies, there are also indications of an interaction between the two phenomena.

It appears thus that the presence of a device capable of 'disrupting' the vortex shedding and controlling the flow structure should be able to impose a much steadier flow in the separated region.

A control method that was reported to be of satisfactory success in bibliography is the porous wall method [7, 8], that allows to stabilize the flow by reducing the unsteadiness. Other ways of controlling the separated region are an acoustic control focused on the separation point, [1, 3] or modulated fluid jets exiting the separation point [6]. The latter method produces a regularization of the vortex shedding and thus a flattening of the whole field unsteadiness.

These controls, though, have the drawback that they require significant increases in design complexity; it is therefore desirable to obtain other control methods that allow a comparable effectiveness through simpler designs.

Within the research project going on at CNR-CSDF in cooperation with DIASP-

Politecnico di Torino and aimed at reaching a better understanding of the origins of separated regions unsteadinesses and to the control of these phenomena, [17, 18, 20], one such method has been tested and will be here described. In particular, this method consists in a LEBU[1]-like device mounted inside the separated shear layer region. The LEBU technique has been studied in the past years for different applications, as it was shown that it can provide drag reduction (see for instance [10, 15]), modifications of heat exchange properties [11, 13] and pressure drop reduction [9] in wall bounded shear flows.

The configuration tested in the present work was a LEBU-like device mounted inside the separated shear layer region. The device is supposed to influence the formation of the shear layer vortices and the backward moving separated structures. The configuration is sketched in Fig. 2, where it is also possible to observe the reference frame employed; X and Y indicate the coordinate system, centered at the step foot. ΔX and ΔY indicate, respectively, the position of the LEBU-like device leading edge lower end, T represents its thickness and C is its chord length.

It will be shown that the control device presented here evidences a large influence on the flow behavior both in terms of mean and fluctuating wall shear stress distributions. The effects of the positioning of the SCB with respect to the step corner on both these quantities will be reported. Because of the working principle, which only in part is analogous to the LEBU one and because of the different aims and outcomes, the device will be here called a 'Separation Control Blade' (SCB).

2 Experimental Setup

Flow visualizations were carried on in a water tunnel in order to provide qualitative information about the flow behavior; quantitative measurements were performed in a rectangular

---

[1]Large Eddy Break Up.

airflow channel. The water tunnel has a vertical test chamber with 25 cm × 25 cm square section, 150 cm long, in which the model is placed. The model consists of a plexiglass bulk shaped in such a way to produce a smooth section reduction followed by a sudden expansion, i.e. a step, 1 cm high, see Fig. 3. The flow was
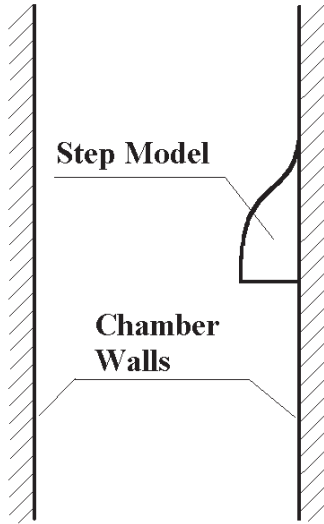

Fig. 3 Sketch of the step in the vertical water tunnel.

seeded with ......μm diameter .... particles and illuminated with a light blade; the visualizations were recorded via a 512 × 768 pixel digital camera.

The air channel is 8 m long and has a section of 7×30 cm^2. Although the channel has an aspect ratio of 4.3 only, a survey of the velocity and turbulence profiles [14] showed that the flow behavior in the centerline section is representative of a two-dimensional channel flow. The step is located 5.9 m downstream of the inlet section, where the channel flow is fully developed (frozen), and is 22 mm high. Thus, the ratio between the step width and height is of 13.6, which allows (see e.g. [4]) to assume the actual separation to be representative of a 2D separation in the channel central section.

The lower wall of the air tunnel downstream of the step was machined in order to insert a sled in the central section. The sled is

6 cm wide; care was taken in order to ensure continuity with the surrounding wall. The sled is driven by two Teflon tracks which allow it to move while ensuring airtightness and is provided with a hole in which a skin friction probe can be mounted flush to the wall; a static pressure tap is also inserted at the same X position, about 1 cm spanwise from the skin friction hole. This structure allows positioning of the measuring devices from 6 mm to 450 mm downstream of the step. A sketch of the step with the sled is presented in Fig. 4.
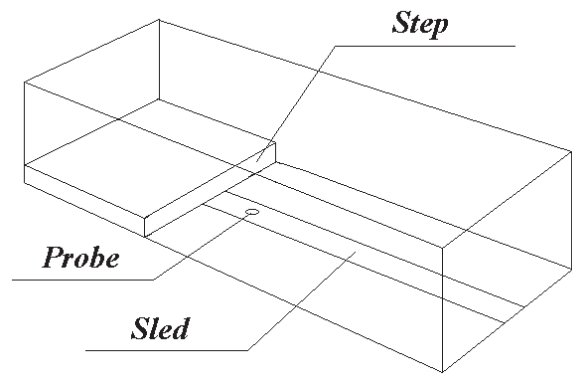

Fig. 4 Sketch of Channel 2 in the step region.

The manipulator tested in the present work, positioned at zero incidence, was a flat brass ribbon 1 mm thick with a chord of 22 mm, i.e. 1 step height. A wide field of the ribbon positioning was examined. Some of the corresponding results, as reported in Table 1, will be discussed in the present paper.

Case number	ΔX (step heights)	ΔY (step heights)
1	0.5	1
2	1	1
3	2	1
4	3	1

Table 1 Manipulator positioning in the different cases.

Skin friction time-resolved measurements were obtained by a special wall mounted

double-hot-wire probe. Full description of the probe design, working principle, properties and validation tests performed on it can be found in [19]. A brief recall of them will be provided here.
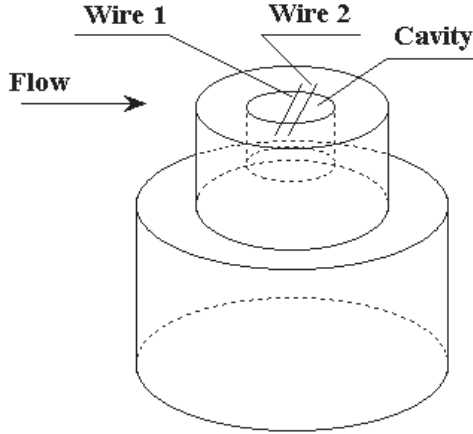

Fig. 5 Sketch of the skin friction probe.

The probe, depicted in Fig. 5, consists essentially of two parallel 5μm diameter tungsten hot wires stretched over a small (1 mm deep $\times$ 1 mm diameter) cavity in the wall where the skin friction is to be measured. The wires are operated through two high precision CTA bridges. The circulation flow induced inside the cavity by the shear stress originating from the external flow will have different intensities and signs depending on the properties of the shear stress itself; by simultaneously measuring the signals from the two wires, it will then be possible to deduce the absolute value and the sign of the shear stress vector.

In the present experiment, the skin friction probe's wires were driven by two AA Lab Systems Ltd. AN1003 CTA bridges; the voltage signals they provided were gathered by a National Instruments 16-bit PCI-MIO-16XE-10 acquisition board connected to a N.I. SC-2040 sample-and-hold module. In each measurement point data were sampled at 4096 Hz for a total acquisition time of 128 s.

3 Experimental Results

The SCB technique was tested first of all in the waterfall tunnel.

In Fig. 6 a sequence of flow visualization images for Case 1 ($\Delta X = H$, $\Delta Y = H$) at a Reynolds number of approximately 3000 is presented. Time intervals scaling is based on step height and external velocity ($\approx$ 30 cm/s). Although it is difficult to understand the flow behavior from still images, dynamical observation of the recordings showed considerable differences with respect to the unmanipulated case. The presence of the manipulator determines a more stable flow configuration, in which both the primary and the secondary bubbles are characterized by almost constant size and position. Moreover, the reattachment length seems to be also influenced by the SCB; indeed, the mean reattachment point seems to be farther from the step than in the unmanipulated case.

These results were substantiated by the quantitative measurements performed in the air channel flow. The data gathered were elaborated in order to obtain statistical values about the skin friction distribution downstream of the BFS and will be presented in terms of mean $C_f = \frac{\overline{\tau_W}}{0.5\rho U_{ref}^2}$ (skin friction coefficient) and of τ'_{RMS} (root mean square value of the fluctuating wall shear stress) as functions of the downstream distance. From the same data, skin friction Fourier spectra have also been computed.

The downstream distance was nondimensionalized to the reattachment length, defined as the mean reattachment point, as previous works (see e.g. [19, 20]) showed that this is the most appropriate scaling length. Moreover, in order to obtain a more clear comparison, the abscissae in the manipulated case were scaled to the unmanipulated case reattachment length. The reattachment length can be inferred from wall shear stress measurements through several methods, [12, 20]. In the present work, the zero-mean-C_f method
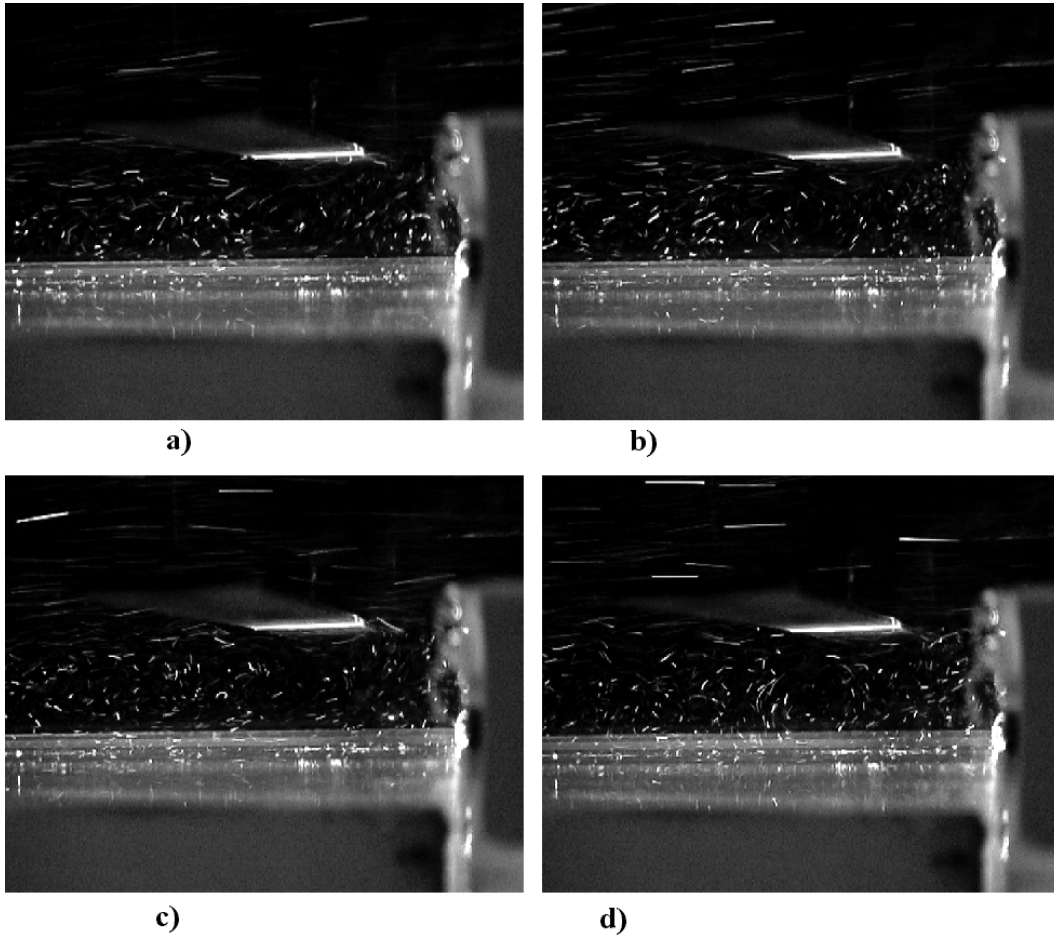
Fig. 6 LEBU-like device flow control visualizations. $\Delta t^*_{a,b} \approx 3$; $\Delta t^*_{b,c} \approx 27$; $\Delta t^*_{c,d} \approx 3$.

was used, as it was shown in the above cited works that it causes no more uncertainty than other methods and it could be readily applied to the data.

First of all, in Fig. 7 the 'reference' results, i.e. the ones obtained without manipulation, are presented together with C_f results obtained by Le et al. [12] via DNS at approximately the same Reynolds number. Remark that the τ'_{RMS} was divided by 5 in order to keep the scales coherent. Observe the satisfactory coherence between the measured results and the DNS data. For representation convenience, the test cases of Table 1 will be plotted in two separate groups, namely results with the SCB 'close' to the step (Cases 1 & 2) or 'far' from it (Cases 3 & 4). Fig. 8 reports the C_f distribution of the former group.

The reference data are represented by the solid line, while the symbols refer to the controlled flow. It can readily be observed that the influence of the manipulator on the separated flow is of paramount importance. The first part of the separated region, up to $\frac{X}{X_R} \approx 0.4$, seems to be only slightly influenced by the manipulation. Soon after this distance though, the C_f distribution changes radically as the SCB is introduced and as its position changes. The flow structure is completely altered; indeed, the mean skin friction distribution exhibits more than one negative peak, indicating thus that the primary bubble is changing to a more complex structure. For both positions in Fig. 8, the reattachment length is increased by more than 20 % and shows a tendency to increase as ΔX is increased. Also, comparing

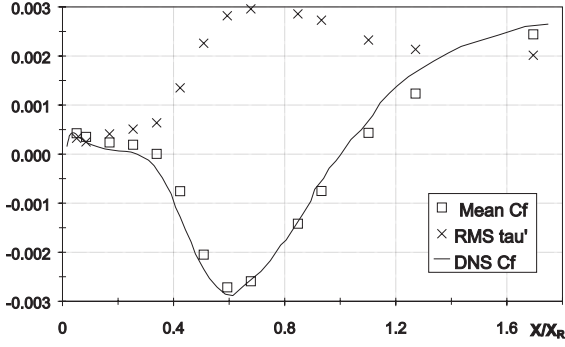**Fig. 7** Skin friction properties downstream a BFS, $Re_H \approx 5100$. Thick solid line, C_f data from [12]; squares, reference C_f from the present work; crosses, reference $\tau'_{RMS} \times 0.2$ from the present work.
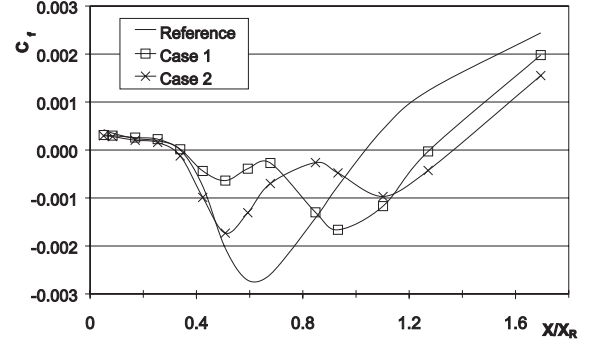

Fig. 8 Skin friction distribution downstream a BFS, $Re_H \approx 5100$. Thick solid line, reference C_f; squares, C_f in Case 1; crosses, C_f in Case 2.

Case 1 to the unmanipulated flow, the absolute value of the C_f is reduced of up to 90 % for $\frac{X}{X_R} \approx 0.65$, while higher values of skin friction are present in the region of the second negative peak.

When attention is focused on the shear stress fluctuation, the results are even more remarkable (Fig. 9). With respect to this quantity, the region immediately downstream the step ($\frac{X}{X_R} \leq 0.4$) again doesn't show appreciable variation in distribution, although lower values of τ'_{RMS} are present. More downstream, in Case 1 it is possible to observe a flow region ($0.5 \leq \frac{X}{X_R} \leq 0.9$) of low fluctuation, with a maximum reduction of ≈ 70 % for $\frac{X}{X_R} \approx 0.7$, followed by an increase that reach to values higher than the ones measured in the unmanipulated case for $\frac{X}{X_R} \geq 1$. In case 2 conversely, the fluctuations are almost everywhere lower than the reference.

These first results strongly suggest a deep modification of the flow topology itself. Indeed, the visualizations (see Fig. 6) indicate the beginning of a splitup of the primary bubble into two corotating vortices. From the results presented here, it appears that this division of the separated flow into two separated structures might bring to a more regular time behavior of the flow field.

The frequency spectra of the shear stress fluctuations have been computed for all the data points of Figs. 8 and 9. The frequencies have been nondimensionalized to the upstream centerline velocity and the reattachment length ($n = \frac{fX_R}{U_0}$). In Fig. 10 a) and b) spectra of the wall shear stress fluctuations for Cases 1 & 2, as well as the corresponding ones for the unmanipulated case, are reported. Examples of spectra are reported for two different distances, namely $X/X_R \approx 0.085$ (Fig. 10 a), which falls in the region of weak influence, and $X/X_R \approx 0.85$ (Fig. 10 b), where conversely an important modification to the flow is produced by the manipulator. Very close to the step (Fig. 10 a), when the ribbon is placed at $\Delta X = 0.5H$ (Case 1), a considerably lower energy content is present at all frequencies with respect to the reference case; on the other side, small benefit is evident up to $n \approx 1$ when the manipulator is at $\Delta X = H$ (Case 2). The effects of manipulation are remarkably different farther from the step, Fig. 10 b): for the whole range of frequencies, both SCB positions cause a reduction of energy levels, but this time the better results are obtained when the manipulator is at the higher distance from the step.

Switching now to the cases in which the ribbon is farther from the step edge, the observable effects on the flow topology are even
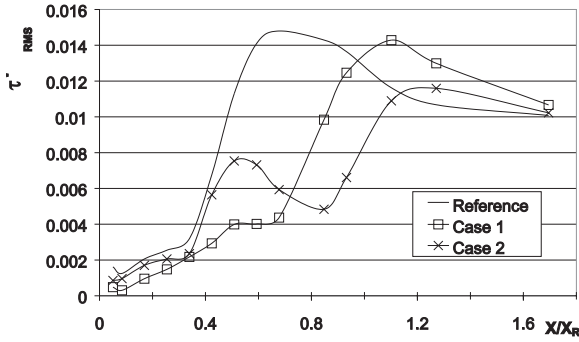
Fig. 9 τ'_{RMS} distribution downstream a BFS, $Re_H \approx 5100$. Thick solid line, reference: squares, Case 1; crosses, Case 2.

Fig. 10 Skin friction frequency spectra, adimensionalized frequency, Cases 1 & 2: a), $X = 10$ mm ($X/X_R \approx 0.085$), b), $X = 100$ mm ($X/X_R \approx 0.85$.)

more evident. In Fig. 11, the C_f distribution in Cases 3 ($\Delta X = 2H$) & 4 ($\Delta X = 3H$) are reported. In these cases again, the control effects are more intense for $\frac{X}{X_R} \geq 0.4$; the C_f distribution shows more similarities to the unmanipulated case than for the previous group of results. Great differences are on the other side observable much farther from the step, $\frac{X}{X_R} \geq 0.8$: indeed, especially when the manipulator is placed at $\Delta X = 2H$, the flow region extending from $\frac{X}{X_R} \approx 0.8$ to $\frac{X}{X_R} \approx 1.3$ shows a very peculiar behavior, being characterized by a vanishing skin friction coefficient. The maximum C_f negative value is increased in both Cases and is reached for lower abscissae; the reattachment length is reduced by approximately 20% in Case 4, while in Case 3 it is difficult to determine a mean reattachment point as the whole region $0.8 \leq \frac{X}{X_R} \leq 1.3$ has its typical behavior. Visualizations for this case showed a very quiet region. This finding is confirmed by the results of Fig. 12, where the τ'_{RMS} distributions for the same Cases are reported. Indeed, it is possible to observe in the whole region $0.8 \leq \frac{X}{X_R} \leq 1.3$ a huge reduction (in some instances by a factor higher than 3) of fluctuation with respect to the baseline case. In particular, the fluctuations in this Cases are almost everywhere lower than the one measured without controls. Moreover, in both Cases the relaxation to the ordinary
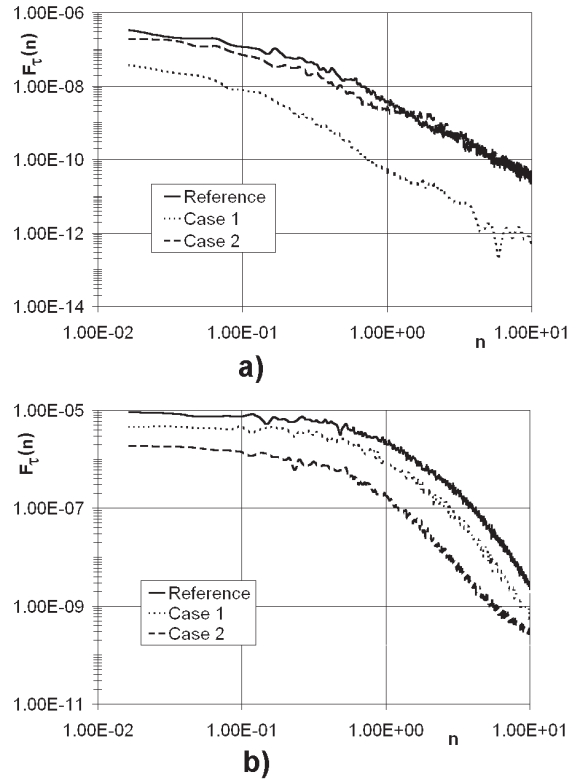
boundary layer flow downstream of the separated region takes an entirely different behavior from the unmanipulated case and from Cases 1 & 2. Indeed, for the 'distant' SCB cases, the relaxation takes place from *lower* values to the asymptote, while in all other instances it comes from *higher* values.

For what concerns the frequency distribution, Fig. 13 reports the energy spectra measured in Cases 3 & 4 at the same positions downstream the step as the ones showed for Case 1 & 2, i.e. $X/X_R \approx 0.085$ and $X/X_R \approx 0.85$. It can be seen in Fig. 13 a) that, just behind the step, as ΔX is increased, higher energy levels are present over the whole frequency range, confirming thus the trend emerging from Fig. 10 a); in particular, for $\Delta X = 3H$ (Case 4) the flow exhibits energetic contents even larger than in the unma-
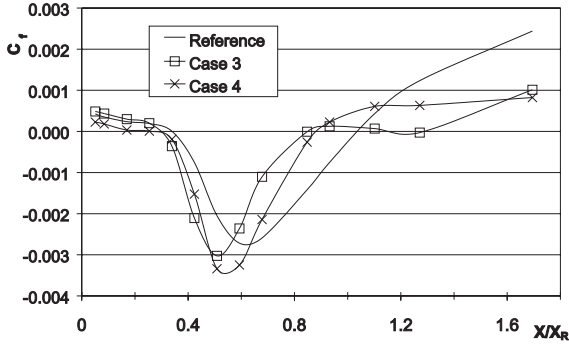
Fig. 11 Skin friction distribution downstream a BFS, $Re_H \approx 5100$. Thick solid line, reference C_f; squares, C_f in Case 3; crosses, C_f in Case 4.

Fig. 12 τ'_{RMS} distribution downstream a BFS, $Re_H \approx 5100$. Thick solid line, reference: squares, Case 3; crosses, Case 4.

nipulated case for all frequencies. Close to the reattachment region ($X/X_R \approx 0.85$, Fig. 13 b) the effects of the manipulator are completely different, as for both manipulated conditions a global energy reduction is evident for all frequencies. Better results are here obtained for the Case 3 configuration, which as already stated, see discussion of Figs. 11 and 12, gives rise to a large region of almost zero friction and very low fluctuations.

4 Conclusions

A first exploratory analysis of a LEBU-like device effects on the behavior of BFS separated flow was conducted. The manipulated flow structure strongly depends on the manipulator positioning. Two regions are essentially present: the first one, close to the step ($X/X_R \leq 0.4$), in which the effects of manipulation are small for the tested blade positions; the second one, farther from the step ($X/X_R \geq 0.4$), where on the other side the effects are much stronger and depend very much on the SCB positioning. Both local skin friction and wall shear stress fluctuations are strongly reduced in the manipulated flow. Flow visualizations showed evidence of the presence of multiple complex structures, much more stable than in the natural flow, within the separated region.
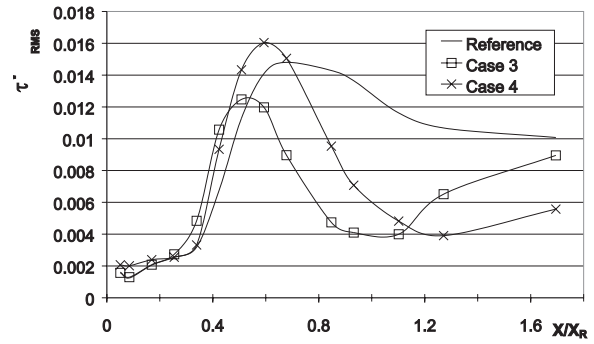
The results are considered to be very promising and work is presently going on in order to identify optimum positions and geometrical configurations for the manipulators. Also, as the underlying fluid mechanics phenomena appear to be quite complex, specific measurements are being prepared in order to clarify the manipulated flow structure.

Acknowledgments

References

[1] S. Bhattacharjee, B. Scheelke, and T. R. Troutt. Modification of Vortex Interactions in a Reattaching Separated Flow. *AIAA Journal*, 24(4):623–629, 1986.

[2] P. Bradshaw and F. Y. F. Wong. The Reattachment and Relaxation of a Turbulent Shear Layer. *Journal of Fluid Mechanics*, 52:113–135, 1972.
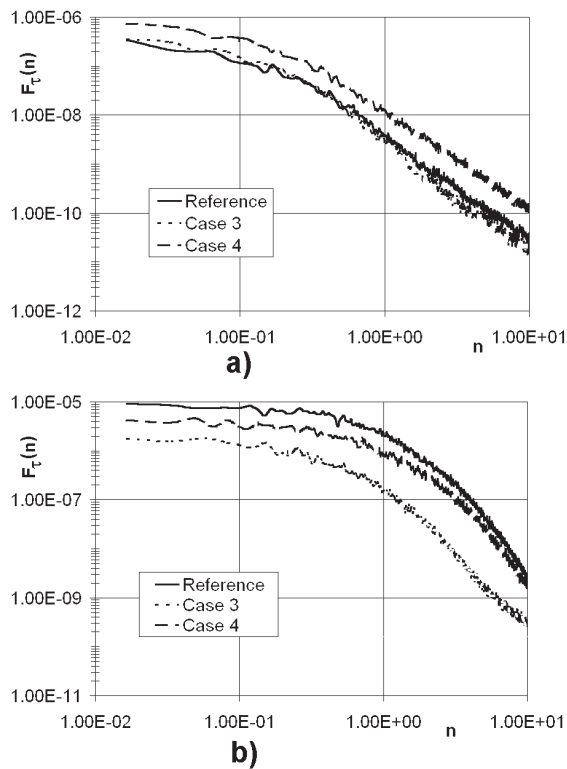
[3] K. B. Chun and H. J. Sung. Control of

Fig. 13 Skin fiction frequency spectra, adimensionalized frequency, Cases 3 & 4: a), $X = 10$ mm ($X/X_R \approx 0.085$), b), $X = 100$ mm ($X/X_R \approx 0.85$).

Turbulent Separated Flow over a Backward-Facing Step by Local Forcing. *Experiments in Fluids*, 21:417–426, 1996.

[4] V. A. S. L. de Brederode and P. Bradshaw. Three-Dimensional Flow in Nominally Two-Dimensional Separation Bubbles. I. Flow behind a Rearward-Facing Step. I.C. Aero Report 72-19, 1972.

[5] J. K. Eaton and J. P. Johnston. A Review of Research on Subsonic Turbulent Flow Reattachment. *AIAA Journal*, 19(9):1093–1100, 1981.

[6] M. A. Z. Hasan. The Flow Over a Backward-Facing Step Under Controlled Perturbation: Laminar Separation. *Journal of Fluid Mechanics*, 238:73–96, 1992.

[7] A. F. Heenan and J. F. Morrison. Passive Control of Pressure Fluctuations Generated by Separated Flow. In *Proceedings of the*

*AIAA 34*th *Aerospace Sciences Meeting and Exhibit*, Reno, Nv., 1996.

[8] A. F. Heenan and J. F. Morrison. Passive Control of Pressure Fluctuations Generated by Separated Flows. *AIAA Journal*, 36(6):1014–1022, 1998.

[9] G. Iuso. Turbulence structure manipulation in a channel flow by outer layer devices. *The Aeronautical Journal*, 98(980):388–394, 1994.

[10] G. Iuso and M. Onorato. Turbulent boundary layer manipulation by outer layer devices. *Meccanica*, 30(4):359–376, 1995.

[11] G. Iuso, M. Onorato, G. M. Carlomagno, L. De Luca, and G. Cardone. Wall Heat Flux Reduction by Outer Layer Devices. In *Proceedings of the 7*th *International Symposium on Flow Visualization*, Seattle, WT., USA, 1995.

[12] H. Le, P. Moin, and J. Kim. Direct Numerical Simulation of Turbulent Flow over a Backward-Facing Step. *Journal of Fluid Mechanics*, 330:349–374, 1997.

[13] E. Marumo, K. Suzuki, and T. Sato. Turbulent heat transfer in a flat plate boundary layer disturbed by a cylinder. *International Journal of Heat and Fluid Flow*, 6(4):241–248, 1985.

[14] M. Onorato Jr., R. Camussi, and G. Iuso. Small-scale intermittency and bursting in a turbulent channel flow. *Physical Review Letter E*, pages –, 2000.

[15] A. M. Savill and J. C. Mumford. Manipulation of turbulent boundary layers by outer-layer devices: Skin friction and flow visualization results. *Journal of Fluid Mechanics*, 191:389–417, 1988.

[16] R. L. Simpson. Turbulent Boundary-Layer Separation. *Annual Review of Fluid Mechanics*, 21:205–234, 1989.

[17] P. G. Spazzini, G. Iuso, M. Onorato, and S. De Ponte. Skin Friction Measurements Downstream of a Back-Facing Step. In *Proceedings of the 21*st *ICAS Congress, A98-31569 ICAS Paper 98-3.10.3*, Melbourne, Australia, 1998.

[18] P. G. Spazzini, G. Iuso, M. Onorato, and A. Mole. DPIV Analysis of Turbulent Flow

over a Back-Facing Step. In *Proceedings of the 8ᵗʰ International Symposium on Flow Visualization, Paper #238*, Sorrento, Italy, 1998.

[19] P. G. Spazzini, G. Iuso, M. Onorato, and N. Zurlo. Design, Test and Validation of a probe for Time-resolved Measurement of Skin Friction . *Measurement Science and Technology*, 10(7):631–639, 1999.

[20] P. G. Spazzini, G. Iuso, M. Onorato, N. Zurlo, and G. M. Di Cicca. Unsteady Behavior of Back Facing Step Flow. *Experiments in Fluids*, 2000? Submitted for Publication.